2025 IEEE World Haptics Conference (WHC)
Suwon Convention Center, Suwon, Korea
July 8 ~ 11, 2025

Influence of Vibrotactile Signal Parameters on Human Perceptual and Behavioral Responses for Forearm-Wearable Devices

Muhammad Akmal Mohammed Zaffir
Division of Information Science
Nara Institute of Science and Technology
Nara, Japan
muhammad.akmal_bin.mb5@is.naist.jp

Sumitaka Honji
Division of Information Science
Nara Institute of Science and Technology
Nara, Japan
honji.sumitaka@naist.ac.jp

Takahiro Wada
Division of Information Science
Nara Institute of Science and Technology
Nara, Japan
t.wada@is.naist.jp

***Abstract*—Wearable vibrotactile devices are increasingly used to communicate robots' states to humans, especially in scenarios requiring physical responses like reaching for handovers. For accurate information transfer, vibrotactile signal design is critical, particularly on the forearm circumference, where anatomical variations may influence perception and behavior. Designing such signals involves selecting appropriate parameter combinations while considering intra-individual and individual variability. However, the influence of signal parameters—such as amplitude (AMP), duration of stimuli (DoS), and inter-stimulus interval (ISI)—on perceptual and behavioral responses across forearm sections remains underexplored. This study addresses this gap by statistically analyzing the relationship between these parameters and human responses across two forearm sections. The findings provide insights for designing practical forearm-wearable vibrotactile systems, enhancing human-machine interaction in applications requiring rapid, precise responses.**

***Index Terms*—Vibrotactile Signals, Wearable Haptic Device, Signal Parameters, Forearm Circumference, Response Surface Methodology.**

I. Introduction

The vibrotactile display method has been used in various applications, such as alerting users to messages on smartphones or smartwatches [1], providing feedback while playing video games on controllers [2], helping visually impaired individuals avoid collisions during navigation [3], and many more. Employing vibrotactile as a communication method elicits faster human response due to the high temporal resolution of the human tactile modality, which allows faster perception compared to visual or auditory modalities [4]. This makes human-machine interaction more efficient. Recently, body-mounted vibrotactile devices have gained popularity in industrial applications, entertainment (e.g., virtual gaming experiences), and communication between humans and robots. These body-mounted devices can convey information such as alerts [5], feedback [6], or contextual signals [7], [8] (i.e., directions).

Several studies focus on the wearable vibrotactile-based haptic device as an interface to communicate robot states to humans for effective collaboration. Some studies have shown that presenting robotic kinematic states on human limbs can help human partners coordinate with robots without relying on visual information [9], [10]. Furthermore, another study proposed a belt-type vibrotactile device with an additional vertical axis on the back of the body to present the absolute position of a robot end-effector [11]. Most recently, Akmal et al. [8] employed an armband-type vibrotactile device to present future robot states. The device presents the robot-intended position as directional cues relative to the forearm during robot-to-human handovers.

To achieve accurate human responses when presenting information using wearable vibrotactile devices, it is crucial to design appropriate vibrotactile signal patterns that can elicit accurate human responses. However, when presenting vibrotactile information on body parts such as the circumference of the forearm, human anatomical variations should be considered, such as differences between muscle-dominated areas and those closer to bones [12], [13], as they can significantly influence the accuracy of how the human perceive and interpret the stimuli (perceptual response) and how human behave in response to the stimuli (behavioral response).

Prior studies have conducted detailed investigations into the impact of signal parameters on human responses [14]–[16]. However, these studies primarily focused on the fingertips or finger area, and their target parameters (e.g., frequency, waveforms, rhythm, etc.) are not commonly used in practical forearm-wearable devices, which rely on simpler parameters such as amplitude, duration of stimuli, and inter-stimulus interval. Additionally, while some studies have demonstrated perceptual differences across sections along the length of the forearm [17], [18] and between the lateral and medial sides of the forearm circumference [19], they did not identify the specific signal parameters influencing these differences. Furthermore, these studies (excluding [19]) focused solely on perceptual responses, leaving a research gap in understanding how signal parameters influence behavioral responses when presented on forearm circumference sections.

To address this gap, this paper investigates the influence

JSPS KAKENHI (Grant Number 24H00298), Japan.

of simple controllable vibrotactile signal parameters on human perceptual and behavioral responses under multivariate changes in different forearm sections. This paper analyzes the effects of the parameters, amplitude (AMP), duration of stimuli (DoS), and inter-stimulus interval (ISI), on the angular directional accuracy when reaching for the presented direction. This paper will address the following research questions:

- Which vibrotactile parameters significantly influence human perceptual and behavioral responses when directional cues are presented on the forearm?
- Is there a difference between human perceptual and behavioral responses to the presented directional cue?
- Is there a difference in perceptual and behavioral responses between different forearm sections where the actuators are placed?

In this paper, Section II describes the methodology used in data collection and analysis. Section III presents the results of the analysis, Section IV discusses the findings in detail, and Section V concludes this study. These sections provide a comprehensive framework for understanding the purpose of this study.

II. Methodology

A. Vibrotactile Device

A forearm-wearable vibrotactile device (Vibroarmband) similar to [8] was developed for this study (Fig. 1a). The device comprised six vibrotactile actuators distributed spatially across the forearm. Each actuator was constructed using an eccentric rotation mass (ERM) vibration motor paired with a haptic driver (Adafruit DRV2605L Haptic Motor Controller) and encased within a 3D-printed body made of ABS material. The actuators were interconnected using a flexible 3D-printed connector crafted from TPU material. A microcontroller (Adafruit QT Py-SAMD21) and a multiplexer (Adafruit PCA9548 8-Channel) were employed to independently control actuators. The device is worn on the right forearm.

B. Vibrotactile Signal Parameters

Our device uses ERM motors due to their practicality. However, modifying the frequency and waveforms with ERM motors is not feasible. Nevertheless, study [20] reported that even with reduced settings, by designing a pulsating vibrotactile signal, the presentation can elicit a better human response than a continuous vibrotactile signal. Therefore, we designed the signals based on the configuration of the amplitude (AMP), duration of stimuli (DoS), and inter-stimulus interval (ISI), as illustrated in Fig. 1b.

We selected three representative values, which are low-, mid-, and high-level values for the experiment. The high-level parameters as shown in Table I, where the AMP value represents the maximum amplitude for the Vibroarmband, and DoS and ISI were set to 500 ms, which is approximately double the human reaction time to vibrotactile stimuli [21]. As for the low-level parameters, we conducted a preliminary investigation on participants to identify their minimum thresholds for AMP and DoS.

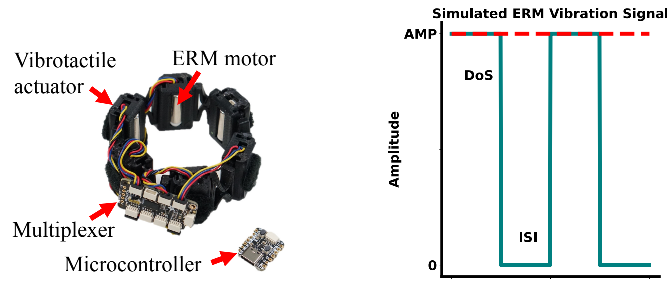

(a) Vibroarmband (b) ERM Vibrotactile signal

Fig. 1: (a) shows the design of the vibrotactile device developed based on study [8]. (b) shows the design of the vibrotactile signal based on the parameters AMP, DoS, and ISI

TABLE I: Signal Parameters

	Low	Mid	High
Amplitude [-]	$x_{1,\text{low}}$	$x_{1,\text{mid}}$	$x_{1,\text{high}} = 127$
Duration of Stimuli [ms]	$x_{2,\text{low}}$	$x_{2,\text{mid}}$	$x_{2,\text{high}} = 500$
Inter-Stimulus Interval [ms]	$x_{3,\text{low}}$	$x_{3,\text{mid}}$	$x_{3,\text{high}} = 500$

The high-level parameter for AMP represents the highest amplitude that the developed device can emits.

C. Minimum Perceptual Threshold Investigation

In this investigation, this paper implemented the method of limits, a widely used psychophysical technique for determining perceptual thresholds. First, the AMP and then the DoS parameters were gradually increased from the lowest possible value until participants detected the stimulus (threshold$_1$). Later, these parameters were gradually decreased from a level above threshold$_1$ until the participant no longer detected the stimulus (threshold$_2$). The low-level parameter is typically calculated as the average of the transition points times by two within each participant (eq. 1).

$$x_{i,\text{low}} = \frac{x_{i,\text{threshold}_1} + x_{i,\text{threshold}_2}}{2} \times 2, \qquad i = 1, 2 \qquad (1)$$

The ISI is set similarly to the DoS. After identifying the low-level thresholds, the mid-level parameters were calculated as the average between the low- and high-level parameters.

D. Experimental Design: Box-Behnken Design

Based on the 3 factorial (parameters) and 3 levels stated in the previous subsection II-B, the combination would lead to a $3 \times 3 \times 3$ complex structure resulting in 27 distinct conditions. To avoid this exhaustive search in the parameter space and reduce the number of combinations, along with analyzing the response based on conditions, this paper employed the response surface methodology (RSM) with a well-known design, the Box-Behnken design (BBD). The BBD reduces the number of conditions to 15. Please refer to [22] for a deeper understanding of BBD and the signal design specification.

E. Participants

A total of 20 participants (10 males and 10 females) with an average age of 27.9 ± 3.82 were recruited for the experiment. One female is left-handed, but all participants are capable of operating a mouse cursor with their right hand. The

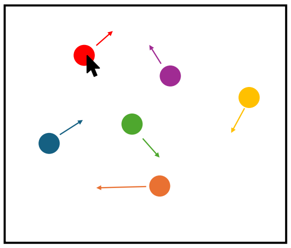

(a) Main task: Track red circle

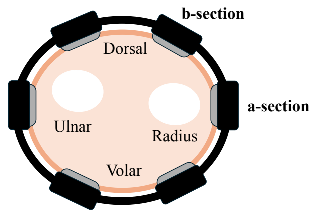

(b) Stimulated forearm section on the circumference

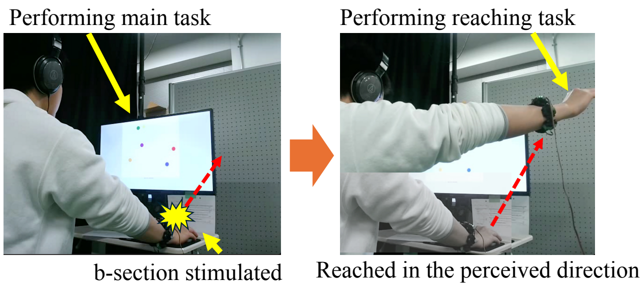

(c) Overview of reaching task execution

Fig. 2: (a) shows the main task performed on a monitor (only the screen is displayed). (b) illustrates the placement of each actuator around the forearm circumference, with forearm sections labeled as a and b. (c) provides an overview of the reaching task execution when the cue is presented during the main task.

research objectives were explained beforehand. Consent was obtained from each participant, and they signed an agreement to participate. They received compensation of 1000 Japanese Yen worth of an Amazon gift card for participating in the experiment. This experiment was approved by the Research Ethics Board of Nara Institute of Science and Technology (no. 2024-I-30).

F. Experiment Protocols

1) Tasks: Participants were required to perform two tasks concurrently. The primary task involved tracking a red circle moving at random speeds among other colored circles on the monitor screen using a mouse placed on the table (Fig. 2a). At random intervals ranging from 5 to 10 seconds, the Vibroarmband (worn on the right forearm) presented a directional cue on one of two sections of the forearm circumference: the a-section or the b-section, as shown in Fig. 2b. Upon perceiving the vibrotactile stimulus, participants were instructed to immediately reach their hand toward the perceived directional cue relative to their forearm, as illustrated in Fig. 2c.

Each participant completed 15 runs (conditions) for each forearm section, resulting in a total of 30 runs with different types of vibrotactile stimuli. The sequence of runs was randomized to prevent participants from anticipating the vibrotactile stimuli. This randomization, along with the concurrent tracking task, was designed to ensure that participants remained focused on the primary task and did not consciously predict the timing or location of the stimuli. One session lasted for approximately 40 minutes, and the participants were given the chance to rest whenever they felt tired during the runs.

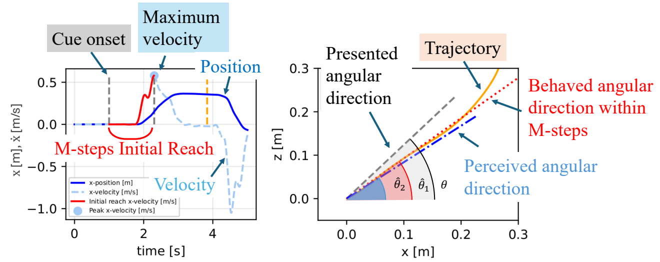

Fig. 3: (Left figure) Plot of the reaching x-position and x-velocity trajectories. The blue line represents the position, and the dashed line represents the velocity on the x-axis. And the red line represents the initial reaching velocity within M-steps. (Right figure) The gray dashed line represents the presented angular direction, the blue dash-dotted line represents the perceived angular direction, and the red dotted line represents the behavioral angular direction within M-steps.

2) Measurements: The human behavioral response measured in this paper was the reaching angular direction in response to the presented angular direction (Fig. 3-right, red dotted line). To extract this value, the reaching trajectory was measured using a motion capture system (s250e series, OptiTrack). Then, we defined the initial reaching behavior within M-steps, which is the range between the cue onset and the point of maximum reaching velocity (Fig. 3-left, between the gray dashed lines). Taking the velocity within that range (Fig. 3-left, red line) on both the x- and z-axis, we calculate the angular position using the following equation:

$$\begin{aligned} \dot{x}_{\text{mean}} &= \text{mean}_M(\dot{x}), \qquad \dot{z}_{\text{mean}} = \text{mean}_M(\dot{z}) \\ \hat{\theta}_b &= \tan^{-1}\left(\frac{\|\dot{z}_{\text{mean}}\|}{\|\dot{x}_{\text{mean}}\|}\right) \end{aligned} \tag{2}$$

where $\text{mean}_M(\cdot)$ denotes the function that calculates the mean of velocity within the range of initial reaching behavior (M-steps), $\dot{x}, \dot{z}$ denote the velocity on the x- and z-axis, respectively, and $\hat{\theta}_b$ denotes the reaching angular direction.

The human perceptual responses are divided into two types, which are the perceived angular direction and subjective scores based on the visual analog scale (VAS). The responses were measured via the questionnaire shown in Fig. 4. Q1 measures the participant's perceived angular direction in response to the presented angular direction on the forearm (a- and b-section) and is denoted as $\hat{\theta}_p$. Q2 and Q3 measure the confidence level in the perceived location on the forearm and the confidence level where participants reached in space, respectively. Q4 measures the stimuli detectability level, and Q5 measures the preference level.

G. Analysis

There are two types of metrics: the perceptual ($\hat{\theta}_p$) and behavioral ($\hat{\theta}_b$) directional squared error and the subjective scores (Q2-Q5). First, the behavioral and perceptual angular directional squared error are computed using the following equation:

$$e_i = (\theta - \hat{\theta}_i)^2, \qquad i = b, p \tag{3}$$

where θ denotes the presented angular direction, $\hat{\theta}$ denotes the responded angular direction, and $i = b, p$ denotes the

Q1	Where did you felt the vibration?	Q2	How **confident** were you to reach in the **direction presented on forearm**?	Low/High
	Mark **[X]** on Figure below	Q3	How **confident** were you to reach in the **direction perceived in space**?	Low/High
		Q4	How **easily** were you able to **perceive the vibration stimuli**?	Hard/Easy
		Q5	How do you **like** the **feeling of the stimuli**?	Dislike/Like

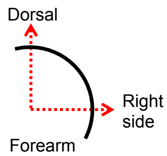

Fig. 4: Questionnaire to measure subjective responses. Q1 asks to mark an 'X' on the figure: Forearm where participants felt the stimuli on their forearm, Q2 asks the confidence in the perceived location on the forearm, Q3 asks the confidence in the reached target in space, Q4 asks the detectability level of the stimuli, and Q5 asks the preference level.

behavioral and perceptual representation of the responded angular direction. Further, the measured subjective scores were transformed into z-scores within their respective participants to ensure comparability. The value is then used for the subjective perceptual responses.

The purpose is to identify the parameters that significantly influence the perceptual and behavioral, as well as their subjective responses, and study the relationship between the parameters and responses. In RSM, quadratic regression models are commonly used to analyze the relationship between the response and predictors. We applied multiple quadratic regression analyses to investigate the linear and curvature relations, along with the influence of parameter interactions on the responses. The three parameters (i.e., AMP, DoS, ISI) are considered independent variables (IVs), while the responses are treated as dependent variables (DVs). Due to the parameter values being calibrated individually, we used the coded value of the IVs instead of the original values. The coded values were calculated as follows:

$$\boldsymbol{X}_{i,c} = \frac{2(\boldsymbol{X}_i - x_{i,\text{mid}})}{x_{i,\text{high}} - x_{i,\text{low}}} \tag{4}$$

where $\boldsymbol{X} = [x_{\text{low}}, x_{\text{mid}}, x_{\text{high}}]^{\text{T}}$ and $i = \text{AMP}, \text{DoS}, \text{ISI}$. The quadratic regression model for the responses can be expressed as follows:

$$Y_i = \boldsymbol{\beta}_i^{\text{T}} \boldsymbol{Z} + \epsilon_i \tag{5}$$

where Y denotes the response and i denotes each DV. $\boldsymbol{Z} = [1, x_1, x_2, x_3, x_1x_2, x_2x_3, x_1x_3, x_1^2, x_2^2, x_3^2]^{\text{T}}$, where $[x_1, x_2, x_3] := [AMP, DoS, ISI]$. $\boldsymbol{\beta} = [\beta_0, \beta_1, \cdots, \beta_9]^T$ denotes the models' coefficients including the intercept (β_0). Finally, ϵ is the error term for the regression models.

III. Results

During the analysis, three participants were excluded from the collected data. Some of the measured data for participants 9 and 10 were lost due to technical issues during the experiment, while participant 16 was excluded due to the behavioral responses being judged as irrelevant to the instructions given during the experiment. Therefore, this section presents the responses and analysis results for 17 participants (8 males and 9 females). Please note that one left-handed female was not excluded.

A. Behavioral and Perceptual Responses

Fig. 5 illustrates the squared angular directional error in both behavioral and perceptual responses across all 15 conditions. Statistical analysis was performed using the Friedman test for each condition, followed by post-hoc analysis with the Wilcoxon signed-rank test. Table II displays the analysis results. The results indicate significant differences between the forearm a- and b-sections for all conditions, except for conditions 2, 3, 6, and 8 in the behavioral response, but no significant differences within the perceptual response for all conditions.

Furthermore, significant differences were observed between the behavioral and perceptual responses in the forearm a-section for conditions 1. For the b-section, significant differences were only found for conditions 4 and 6.

TABLE II: Comparison between forearm sections for behavioral response, between behavioral and perceptual responses for forearm sections a and b.

	Behavioral		Behavioral vs Perceptual			
Forearm	a vs b		a		b	
Runs	z-score	p-val	z-score	p-val	z-score	p-val
1	-4.52	0.040 *	-2.25	0.023 *	-0.83	0.431
2	-4.35	0.120	-1.87	0.064	-1.07	0.306
3	-4.33	0.132	2.82	0.003 **	-0.40	0.712
4	-4.66	0.013 *	-2.91	0.002 **	-2.20	0.027 *
5	-4.78	0.004 **	-1.87	0.064	-0.21	0.854
6	-4.03	0.517	-1.59	0.120	-2.06	0.040 *
7	-4.59	0.023 *	-0.78	0.459	-0.36	0.747
8	-4.30	0.159	-2.25	0.023 *	-1.92	0.057
9	-4.88	0.001 **	-2.53	0.009 **	-0.60	0.579
10	-4.86	0.001 **	-2.86	0.003 **	-0.59	0.579
11	-4.59	0.023 *	-3.05	0.001 **	-0.07	0.963
12	-4.59	0.023 *	-2.72	0.005 **	-1.63	0.109
13	-4.69	0.009 **	-2.39	0.015 *	-0.12	0.927
14	-4.80	0.003 **	-2.39	0.015 *	-0.12	0.927
15	-4.88	0.001 **	-1.63	0.109	-0.21	0.854

The * and ** indicate $p < 0.05$ and $p < 0.01$, respectively.

B. Multiple Quadratic Regression Analyses

Since there were significant differences between the forearm a- and b-section in some responses for some of the conditions, it is wise to see whether the regression models were also significantly different or not. We initially fitted the models for each respective forearm section, a and b. Then, we combined the data and fitted a single model. The sum of squared residuals for sections a, b, and the combined model were extracted, and the Chow test was conducted. The results of the Chow test indicated a significant difference between the regression models for the a- and b-sections in the behavioral response (F = 7.45, $p < 0.001$) and the stimuli detectability response (F = 2.41, $p = 0.011$). Therefore, we fitted the models for these two responses separately within their respective forearm sections and fitted a combined dataset for the other responses. Table III shows the results of the regression analyses.

Fig. 6a illustrates the coefficients and their significance on the responses with significant differences between forearm a- and b-section. For the behavioral response, the vibrotactile parameters show no significant relation on either forearm section. For stimuli detectability in the forearm a-section, both

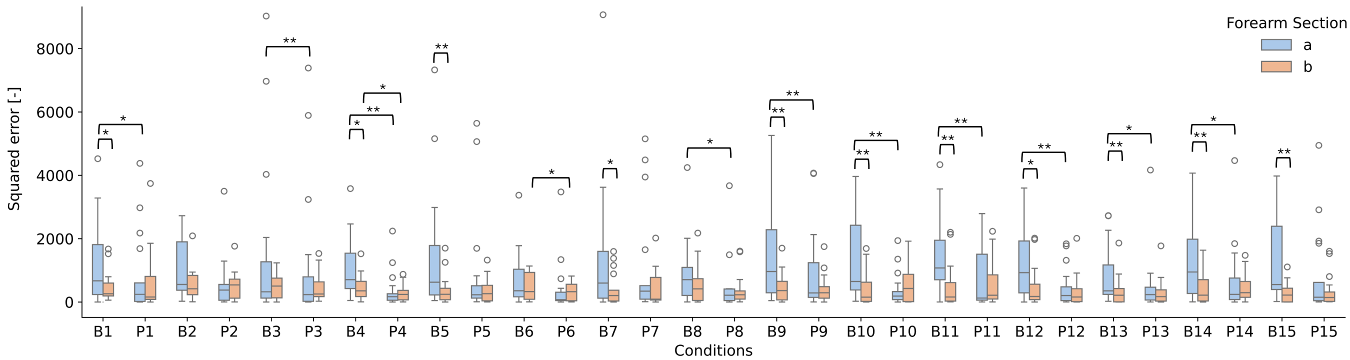

Fig. 5: Graphs show the box plots of the responses, where the horizontal axis represents the 15 conditions (parameter combination based on BBD), and the blue and orange box plots represent the forearm sections a and b, respectively. Both behavioral (B) and perceptual (P) angular squared errors are plotted within the same graph. (e.g., behavioral response for condition 1: "B1", and perceptual response for condition 1: "P1"). The * and ** indicates $p < 0.05$ and $p < 0.01$, respectively.

AMP and DoS exhibit significant positive linear relations. Additionally, both AMP and DoS show concave relations. The interaction between AMP and DoS negatively influences the response. In the forearm b-section, all parameters demonstrate significant linear relations with the response. DoS also shows a significant concave relation, while the interaction between DoS and ISI has a significant positive influence on the response.

Fig. 6b illustrates the remaining responses. For the perceptual response, AMP shows a significant negative linear relation. Regarding the confidence level of the perceived location on the forearm, all parameters show significant linear relations. Additionally, DoS exhibits a significant concave relation, and the interaction between AMP and DoS negatively influences the response. For the confidence level of the perceived target in space, AMP and DoS show significant positive linear relations, while DoS also demonstrates a significant concave relation. Finally, for preference, both AMP and DoS show significant positive linear relations, while DoS exhibits a significant concave relation.

IV. Discussion

A. Effectiveness of Vibrotactile Parameters

The regression model analysis showed that the tested parameters did not significantly influence behavioral response accuracy. However, amplitude (AMP) significantly influenced the perceptual response accuracy, with higher values leading to a decrease in squared error, as illustrated in Fig. 7b. Our results demonstrate a relationship between vibration amplitude and perceived angular direction accuracy across the two target forearm sections on the lateral side, further supporting the results reported in [19].

Additionally, most parameters significantly influenced subjective scores, particularly the duration of stimuli (DoS), which exhibited a critical (maximum) point in the curvature relationship, as shown for confidence levels in Fig. 7c. While previous studies have focused solely on linear relationships [16], the present study incorporates nonlinear aspects of these relationships. This paper identifies the existence of an optimal value for the duration of stimulus that maximizes the perceptual aspect of the response, including confidence level, stimuli detectability, and user preference. These findings offer valuable insights for designing signal parameters that can enhance human performance in vibrotactile interface applications.

B. Behavioral vs Perceptual Responses

The behavioral response results (Fig. 5) indicate that the b-section demonstrates better accuracy compared to the a-section. The Chow test results further confirm a significant difference in behavioral responses between the a- and b-sections. However, the a-section exhibits a large negative error, as the behavioral angular direction exceeded the presented direction (Fig. 7a). Additionally, there was no significant difference in the perceived angular direction error between the a- and b-sections. This suggests that the discrepancy between behavioral and perceptual responses may be influenced by an additional factor. One possible explanation is that participants interpreted the presented angular direction relative to their torso rather than their forearm.

Humans typically use a head- or torso-centered frame of reference for spatial localization, with a stronger reliance on the torso [23]. Thus, when perceiving cues on the forearm, participants may have translated the positions relative to their torso. The lower error in the b-section may be attributed to the alignment between the presented direction and the relative direction from the torso. Therefore, it is essential to further investigate how humans interpret spatial positions when cues are presented on their limbs.

However, other anatomical factors, such as variations in forearm muscle density, hairiness, and skin sensitivity, require further investigation. Additionally, differences in forearm posture during movement should be examined, as they may influence how humans perceive vibrotactile stimuli. Finally, the actual vibration amplitude might be different from the signal intensity, which we would also have to further investigate. Nevertheless, our findings contribute to the ongoing development of forearm-wearable vibrotactile devices by leveraging simple, well-configured signals for practical applications in human-machine communication, particularly in human-robot physical interactions.

TABLE III: Significant relation between independent and dependent variables based on the result of regression analysis (t-value (p-value))

DV	AMP	DoS	ISI	AMPxDoS	DoSxISI	AMPxISI	AMP^2	DoS^2	ISI^2
a_Behavioral squared error	-	-	-	-	-	-	-	-	-
b_Behavioral squared error	-	-	-	-	-	-	-	-	-
a_Std. stimuli detectability	9.06 (†)	7.13 (†)	-	2.38 (0.018)	-	-	6.02 (†)	3.99 (†)	-
b_Std. stimuli detectability	5.55 (†)	6.24 (†)	4.01 (†)	-	2.33 (0.021)	-	-	3.71 (†)	-
Perceptual squared error	2.69 (0.007)	-	-	-	-	-	-	-	
Std. confidence (forearm)	7.16 (†)	5.35 (†)	2.77 (0.006)	2.52 (0.012)	-	3.81 (†)	-		-
Std. confidence (space)	6.55 (†)	4.66 (†)	-	-	-	-	-	3.49 (0.001)	-
Std. preference	2.92 (0.004)	2.24 (0.026)	-	-	-	-	-	2.48 (0.013)	-

Note: Only parameters that significantly influence the dependent variables are shown. † indicates $p < 0.001$ and a dash (–) indicates no significant effect.

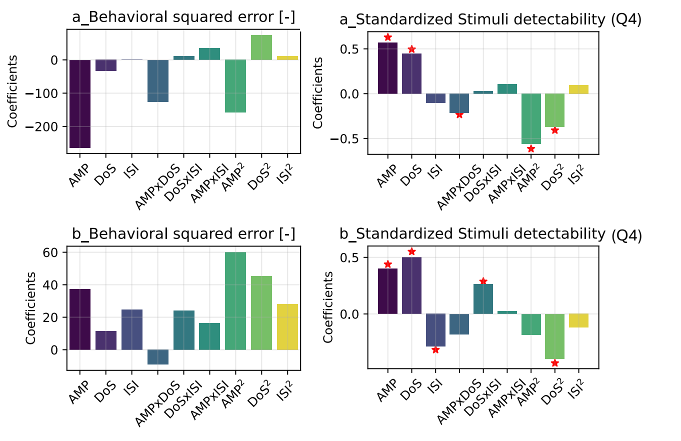

(a) Coefficients of regression models based on forearm sections ($p < 0.05$ based on the Chow test). Top: a-section, bottom: b-section

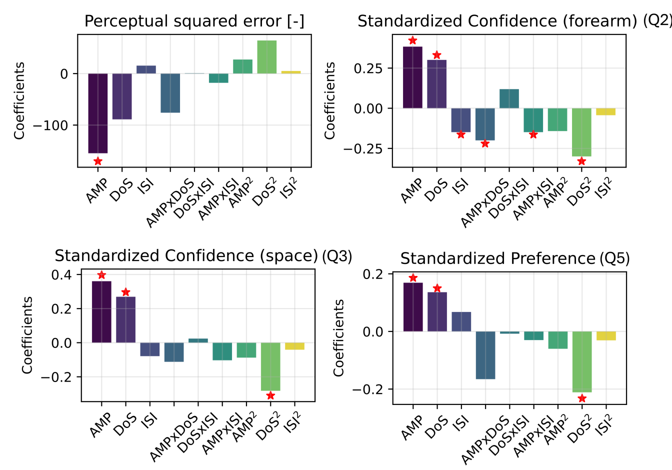

(b) Coefficients of regression models for combined forearm sections ($p \geq 0.05$ based on the Chow test)

Fig. 6: (a) shows the coefficients fitted on the behavioral squared error and stimuli detectability (Q4) models on both forearm a- and b-sections. (b) shows the coefficients fitted on the perceptual squared error, confidence level (forearm (Q2) and space (Q3)), and preference level (Q5) models on combined forearm sections data. This was determined based on the Chow test results (Section III-B).

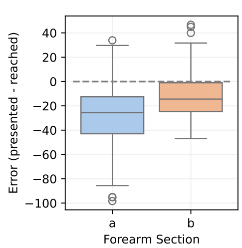

(a) Error between presented and behavioral angular direction

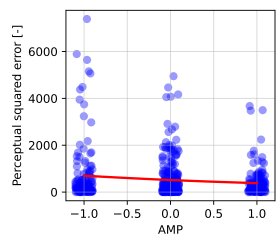

(b) Relationship between amplitude and perceptual squared error

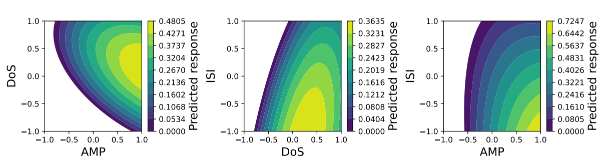

(c) Contour plot: Confidence level (forearm) predicted response

Fig. 7: (a) shows the error between the presented and behavioral angular direction in each forearm section. (b) illustrates an example where the error decreases as AMP increases. (c) displays an example of the response surface for the subjective scores, demonstrating a concave relationship.

V. Conclusion

This paper investigates the effects of vibrotactile parameters on human perceptual and behavioral responses across two distinct forearm regions. A 3-factor, 3-level Box-Behnken design based on response surface methodology was employed to collect data. Multiple quadratic regression analyses were conducted to examine the influence of amplitude (AMP), duration of stimulus (DoS), and inter-stimulus interval (ISI) on the measured responses. The key findings indicate that AMP significantly affects perceptual responses, while AMP, DoS, and ISI do not significantly influence behavioral responses, regardless of forearm region. These parameters also significantly impact subjective ratings on both forearm sections. Finally, differences in behavioral responses between the two regions suggest that different areas of the forearm perceive vibrotactile stimuli differently, although further investigation is needed.

Acknowledgment

This work was partially supported by JSPS KAKENHI (Grant Number 24H00298), Japan.

References

[1] B. Saket, C. Prasojo, Y. Huang, and S. Zhao, ‘Designing an effective vibration-based notification interface for mobile phones’, in Proceedings of the 2013 conference on Computer supported cooperative work, 2013, pp. 149–1504.

[2] X. Tao, K. Wu, and Y. Yang, ‘The effects of vibration on assisting game play and improving player engagement when lacking sound’, in International Conference on Human-Computer Interaction, 2021, pp. 389–407.
[3] N. Mahmud, R. K. Saha, R. B. Zafar, M. B. H. Bhuian, and S. S. Sarwar, ‘Vibration and voice operated navigation system for visually impaired person’, in 2014 international conference on informatics, electronics & vision (ICIEV), 2014, pp. 1–5.
[4] A. W. Y. Ng and A. H. S. Chan, ‘Finger response times to visual, auditory and tactile modality stimuli’, in Proceedings of the international multiconference of engineers and computer scientists, 2012, vol. 2, pp. 1449–1454.
[5] S. Sellak, O. Haberchad, S. Ibenyahia, and Y. Salih-Alj, ‘A UWB Vibrotactile Safety Monitoring System for Factory Environments’, in 2023 7th IEEE Congress on Information Science and Technology (CiSt), 2023, pp. 305–310.
[6] V. Villani, G. Fenech, M. Fabbricatore, and C. Secchi, ‘Wrist Vibration Feedback to Improve Operator Awareness in Collaborative Robotics’, Journal of Intelligent & Robotic Systems, vol. 109, no. 3, p. 45, 2023.
[7] J. V. S. Luces, K. Okabe, Y. Murao, and Y. Hirata, ‘A phantom-sensation based paradigm for continuous vibrotactile wrist guidance in two-dimensional space’, IEEE Robotics and Automation Letters, vol. 3, no. 1, pp. 163–170, 2017.
[8] M. A. B. Mohammed Zaffir and T. Wada, ‘Presentation of Robot-Intended Handover Position using Vibrotactile Interface during Robot-to-Human Handover Task’, in Proceedings of the 2024 ACM/IEEE International Conference on Human-Robot Interaction, 2024, pp. 492–500.
[9] A. Noccaro, L. Raiano, M. Pinardi, D. Formica, and G. Di Pino, ‘A novel proprioceptive feedback system for supernumerary robotic limb’, in 2020 8th IEEE RAS/EMBS International Conference for Biomedical Robotics and Biomechatronics (BioRob), 2020, pp. 1024–1029.
[10] M. Pinardi, L. Raiano, A. Noccaro, D. Formica, and G. Di Pino, ‘Cartesian space feedback for real time tracking of a supernumerary robotic limb: A pilot study’, in 2021 10th International IEEE/EMBS Conference on Neural Engineering (NER), 2021, pp. 889–892.
[11] Y. Iwasaki, K. Ando, and H. Iwata, ‘Haptic feedback system of the additional hand position for multiple task situations using a wearable robot arm’, in 2019 IEEE International Conference on Cyborg and Bionic Systems (CBS), 2019, pp. 247–252.
[12] L. A. Jones, ‘Human hand function’. Oxford University Press, 2006.
[13] J. Van der Wal, ‘The architecture of the connective tissue in the musculoskeletal system—an often overlooked functional parameter as to proprioception in the locomotor apparatus’, International Journal of Therapeutic Massage & bodywork, vol. 2, no. 4, p. 9, 2009.
[14] J. W. Morley and M. J. Rowe, ‘Perceived pitch of vibrotactile stimuli: effects of vibration amplitude, and implications for vibration frequency coding’, The Journal of Physiology, vol. 431, no. 1, pp. 403–416, 1990.
[15] I. Hwang, J. Seo, M. Kim, and S. Choi, ‘Vibrotactile perceived intensity for mobile devices as a function of direction, amplitude, and frequency’, IEEE Transactions on Haptics, vol. 6, no. 3, pp. 352–362, 2013.
[16] H. Hasegawa, S. Okamoto, K. Ito, and Y. Yamada, ‘Affective vibrotactile stimuli: Relation between vibrotactile parameters and affective responses’, International Journal of Affective Engineering, vol. 18, no. 4, pp. 171–180, 2019.
[17] N. Yeganeh, I. Makarov, R. Unnthorsson, and Á. Kristjánsson, ‘Effects of stimulus frequency and location on vibrotactile discrimination performance using voice coil actuators on the forearm’, in Actuators, 2023, vol. 12, p. 224.
[18] A. Barghout, J. Cha, A. El Saddik, J. Kammerl, and E. Steinbach, ‘Spatial resolution of vibrotactile perception on the human forearm when exploiting funneling illusion’, in 2009 IEEE International workshop on haptic audio visual environments and games, 2009, pp. 19–23.
[19] C.-Y. Ko et al., ‘Evaluation of physical and emotional responses to vibrotactile stimulation of the forearm in young adults, the elderly, and transradial amputees’, Physiology & Behavior, vol. 138, pp. 87–93, 2015.
[20] M. A. B. Mohammed Zaffir and T. Wada, ‘Presenting Human-Robot Relative Hand Position using a Multi-Step Vibrotactile Stimulus for Handover Task’, in Companion of the 2023 ACM/IEEE International Conference on Human-Robot Interaction, 2023, pp. 426–430.
[21] D. J. Caldwell et al., ‘Direct stimulation of somatosensory cortex results in slower reaction times compared to peripheral touch in humans’, Scientific Reports, vol. 9, no. 1, p. 3292, 2019.
[22] S. L. C. Ferreira et al., ‘Box-Behnken design: an alternative for the optimization of analytical methods’, Analytica chimica acta, vol. 597, no. 2, pp. 179–186, 2007.
[23] M. R. Longo, S. S. Rajapakse, A. J. T. Alsmith, and E. R. Ferrè, ‘Shared contributions of the head and torso to spatial reference frames across spatial judgments’, Cognition, vol. 204, p. 104349, 2020.